Materials Research. 2015; 18(Suppl 2): 35-38
DOI: http://dx.doi.org/10.1590/1516-1439.338914
© 2015

Phase Formation, Thermal Stability and Mechanical Properties of a Cu-Al-Ni-Mn Shape Memory Alloy Prepared by Selective Laser Melting

Piter Gargarella[a]*, Cláudio Shyinti Kiminami[a], Eric Marchezini Mazzer[b], Régis Daniel Cava[a], Leonardo Albuquerque Basilio[a], Claudemiro Bolfarini[a], Walter José Botta[a], Jürgen Eckert[c,d], Tobias Gustmann[c], Simon Pauly[c]

[a]*Departmento de Engenharia de Materiais, Universidade Federal de São Carlos – UFSCar, São Carlos, SP, Brazil*
[b]*Programa de Pós-graduação em Ciência dos Materiais e Engenharia, Universidade Federal de São Carlos – UFSCar, São Carlos, SP, Brazil*
[c]*Institute for Complex Materials – IFW Dresden, Dresden, Saxónia, Germany*
[d]*Institute of Materials Science, Dresden University of Technology – TUD, Dresden, Saxónia, Germany*

Received: October 27, 2014; Revised: July 28, 2015

Selective laser melting (SLM) is an additive manufacturing process used to produce parts with complex geometries layer by layer. This rapid solidification method allows fabricating samples in a non-equilibrium state and with refined microstructure. In this work, this method is used to fabricate 3 mm diameter rods of a Cu-based shape memory alloy. The phase formation, thermal stability and mechanical properties were investigated and correlated. Samples with a relative density higher than 92% and without cracks were obtained. A single monoclinic martensitic phase was formed with average grain size ranging between 28 to 36 μm. The samples exhibit a reverse martensitic transformation temperature around 106 ± 2 °C and a large plasticity in compression (around 15±1%) with a typical "double-yielding" behaviour.

Keywords: *selective laser melting, shape memory alloys, Cu-based alloys, additive manufacturing*

1. Introduction

Selective laser melting (SLM) is a versatile additive manufacturing process. Parts are built layer by layer, which allows customizing their density and obtaining complex shapes[1]. A large number of processing parameters can be varied as laser power, scanning speed, spot size and overlapping of individual tracks (hatching)[1]. This makes necessary to investigate the best combination of parameters in order to produce samples with particular properties, as for example, high density and with a refined microstructure.

This method was barely used to fabricate shape memory alloys (SMAs)[2,3]. These alloys have the ability to recover their initial shape after plastic deformation by means of a structural transformation upon heating to a critical temperature. A low symmetry phase (martensite) undergoes a reverse martensitic transformation to a high-temperature phase (parent phase). SMAs are used in several applications including pipe couplings, orthodontic wires, micro-actuators, and a variety of biomedical devices[4]. The Cu-based SMAs have some advantages when compared with traditional TiNi-based SMAs because they have larger thermal and electrical conductivities, have a lower cost and are easier to process[5].

As a drawback, Cu-based SMAs have a reduced recoverable strain and a low ductility at room temperature due to intergranular cracking[5], which is related to an abnormally high elastic anisotropy, particularly when large grains are present. The high cooling rate applied during the SLM process promotes a grain refinement, which could help to improve the ductility and fatigue behaviour[6]. Moreover, the performance of SMA components strongly depend on the microstructure, i.e. the phases present, their distribution and their respective sizes[7]. It is important to verify how the grain refinement and the non-equilibrium state promoted by the SLM process affect the properties of SMAs including their thermal stability and mechanical properties.

The present work aims to investigate the correlation between phase formation, thermal stability and mechanical properties of a Cu-Al-Ni-Mn shape memory alloy produced using an innovative processing route that combines SLM and gas atomization.

2. Experimental Procedure

Gas-atomized powders of the Cu-11.85Al-3.2Ni-3Mn (wt%) alloy were prepared by nitrogen gas atomization. The parameters used and the description of the set up can be found elsewhere[8,9]. Powders with size in the range 32 to 106 μm were used to produce rods with 3 mm in diameter and 10 mm in length on a Cu10%Sn substrate using a SLM device (SLM Solutions GmbH, model SLM 250 HL). The nominal composition of the powders was confirmed by

*e-mail: piter@ufscar.br

energy-dispersive X-ray spectroscopy (EDX). The processing was carried out in an inert argon atmosphere using a Laser Nd-YAG. The parameters used were previously optimized in order to have high relative densities[9]. The power, scanning speed and hatching used were 300 W, 500 mm/s and 50%, respectively.

The structure of the rods was investigated by X-ray diffraction (XRD) in a Rigaku ME210GF2 with Cu-Kα radiation and in a STOE STADI P with Mo-Kα radiation and the microstructure was studied using a Philips XL 30 FEG and a Hitachi Tabletop Microscope TM-1000 scanning electron microscopes. The thermal stability of the samples was analyzed by differential scanning calorimetry (DSC) with a DSC 7 PerkinElmer using a heating rate of 10 K/min. The pores distribution was determined by X-ray tomography using a Phoenix Nanotom General Electrics. The density of the rods was also measured using the Archimedes principle.

The mechanical properties of the rods were measured by compression tests using an INSTRON 5869. The samples have 3 mm in diameter and 6 mm in length and the strain rate used was 0.001 s^{-1}. The strain was measured with a laser extensometer Fiedler Optoelektronik.

3. Results and Discussion

The morphology of the powder used can be seen in Figure 1. There is a mix of particles with spherical and non-spherical shape. The particles with non-spherical shape probably solidified only when their movement was interrupted by the atomization chamber, which modifies the shape from spherical to more ellipsoidal. The XRD result (inset Figure 1) proves that only the β'-martensite (a = 0.443 nm, b = 0.530 nm, c = 1.278 nm and β = 95.8°, with space group P21/m[10]) was formed in the powder. The powder selected to be used has particles size < 106 μm, with 60% in the range 75 – 106 μm.

The powder was then used to produce 3 mm diameter rods (inset Figure 2a) by SLM. The rods exhibit a similar XRD pattern to the powders (inset Figure 1) with only the β'-martensite being detected. No cracks were observed in the rods but they exhibited a poor surface quality (inset Figure 2a), which is probably related to the large particles size used (< 106 μm). The rods microstructure was investigated using SEM and the results are shown in Figure 2. Grains

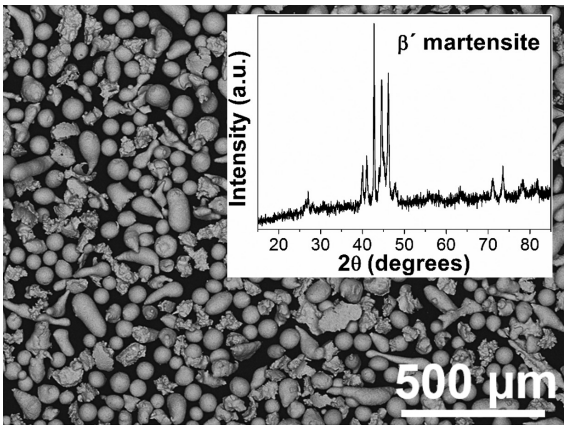

Figure 1. SEM image of the powder with size in the range 45 – 75 μm. Spherical and non-spherical particles are seen. The inset shows the XRD result for this powder, proving that only the β'-martensite is formed.

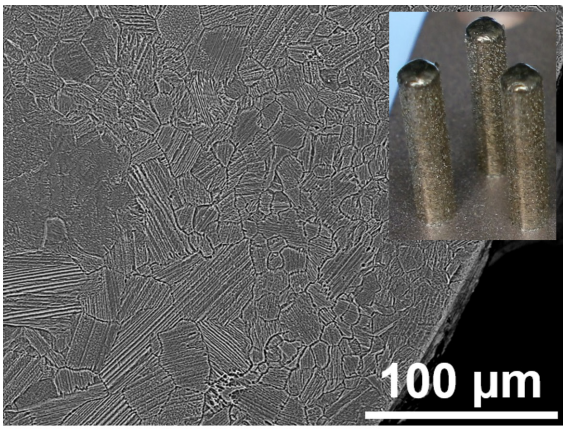

(a)

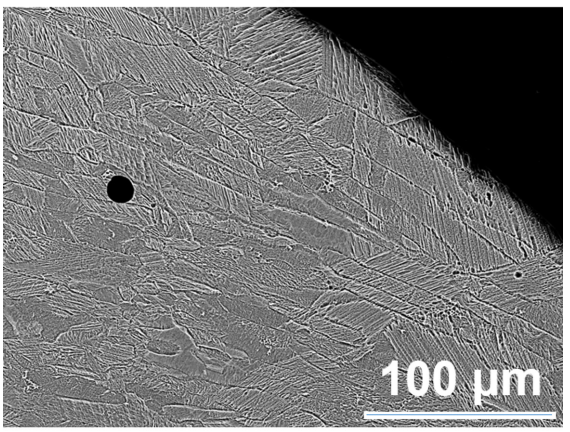

(b)

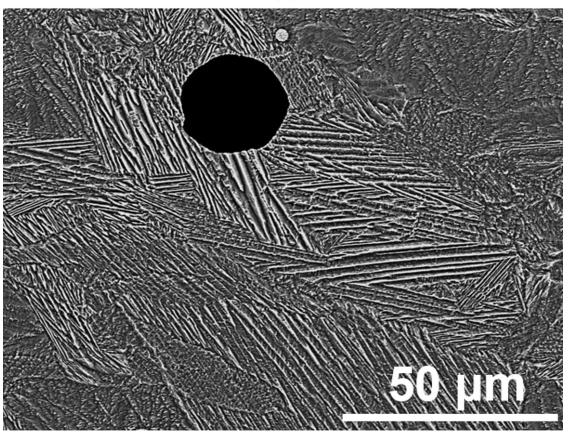

(c)

Figure 2. SEM micrographs of a rod produced by SLM. (a) Cross section of the rod, showing grains with equiaxial morphology and a heterogeneous size distribution. The inset shows the rods produced by SLM. (b) Longitudinal section of the rod. Elongated grains are formed in the direction of the heat extraction. (c) Cross section showing the zigzag morphology of the martensite and the formation of spherical pores in the samples.

with a heterogeneous size distribution and average grain size between 28 (cross section) and 36 μm (longitudinal) were formed (Figure 2a). The grain size was measured using Equation 1[11]:

$$d = 2\sqrt{\frac{S}{\pi N}} \quad (1)$$

where S is the area of a certain circle defined at a micrograph and N is the effective number of grains inside this circle.

The grains exhibit an elongated morphology at the longitudinal section of the rod, following the direction of heat extraction from top to bottom (Figure 2b). The martensite formed in the samples exhibits the zigzag morphology typical of the β' martensite (Figure 2c), which corroborates with the XRD results, and consists of fine martensite laths with thickness varying from 50 to 200 nm. The density measured by the Archimedes method was 6,826 g/cm^3, which correspond to 92.4% of the theoretical density (7,390 g/cm^3). The relative low density is attributed to the large amount of pores formed in the samples (Figure 2c). Their formation was favored by the non-spherical morphology of the powder used (Figure 1), which probably did not allow a good densification of the powder layer. The pores size varies from 15 to 25 μm and they are homogeneously distributed in the rod as can be seen in the X-ray tomography image shown in the inset of Figure 3.

The mechanical behaviour of the rods was investigated in compression and the results are shown in Figure 3. The rod shows average fracture strain, yield strength and ultimate tensile strength of 15±1%, 113±38 MPa and 1086±30 MPa, respectively. A large work hardening was observed with the ultimate tensile strength almost 10 times larger than the yield strength. A typical "double yielding" behaviour was observed with the presence of two inflection points (indicated by arrows), which correspond to the beginning of martensite reorientation and its plastic deformation, respectively[12]. The relative large plasticity observed is attributed to the microstructural refinement promoted by the selective laser melting processing.

It was observed that some monocrystalline Cu-based SMAs with a martensitic structure can exhibit a superelastic (or pseudoelasticity) behaviour[10], which is a large strain recovery (up to 18%) after unloading[12]. It was performed different load-unload tests in order to investigate the superelastic behaviour of the rods nevertheless, this was not observed probably because they are polycrystals. The grain boundaries usually inhibits this behaviour[12]. Some Cu-based SMAs also exhibit phase transformations during deformation as the Cu-14,0Al-4,2Ni (wt.%) alloy, in which the γ_1' martensite undergoes transformation to the β_1" martensite during loading[5]. The deformed rods were also checked by XRD but no phase transformation occurred.

It is also important to verify the influence of the microstructural refinement in the thermal stability of the alloy. This study was carried out by differential scanning calorimetry and the results are shown in Figure 4. Only a single transformation peak is observed and it corresponds to the martensitic transformation (cubic P2mm structure to monoclinic β'-martensite) as could be inferred by in-situ XRD analyses. The martensitic transformation occurs around 106 ± 2 °C during the reverse (martensite → austenite) transformation. Similar transformation temperatures were observed during three different thermal cycles.

The fracture surface of a rod after compression is shown in Figure 5. The fracture occurs around 45° (inset Figure 5) to the loading direction, in the direction of maximum shear stress. Dimples were seen at the fracture surface (Figure 5),

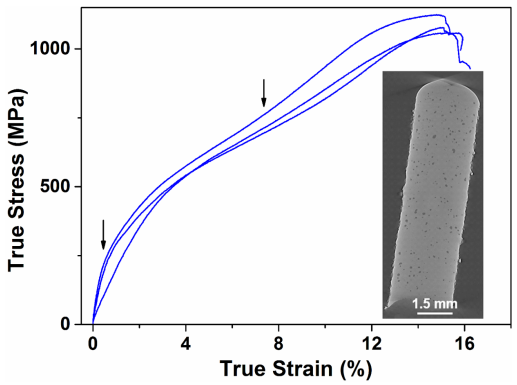

Figure 3. Compression test results for the rods prepared by SLM. Two inflection points are observed (indicated by arrows), which correspond to the "double yielding" behaviour typically observed for shape memory alloys. The inset shows an image obtained by X-ray tomography. A homogeneous distribution of pores is seen.

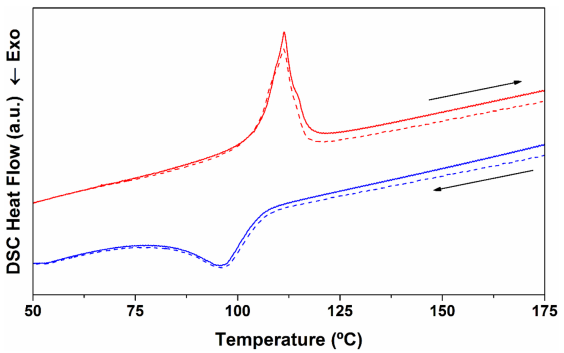

Figure 4. DSC results for the rods. The full lines refer to the first thermal cycle and the dashed refer to the second.

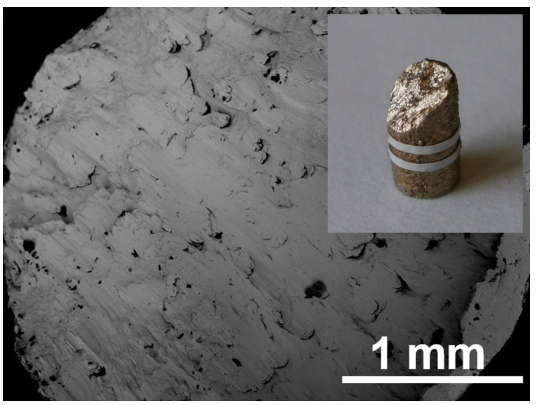

Figure 5. Fracture surface of the rod. Dimples are seen at the surface. The inset shows that the fracture occurred around 45 ° to the loading direction.

which shows that the samples deformed considerably before fracture.

4. Conclusion

The results obtained showed that is possible to produce samples of Cu-based shape memory alloys by the combination of atomization and selective laser melting. The samples exhibited a relative density around 92%, showing a considerable amount of pores as inferred by SEM and X-ray tomography. The large porosity is attributed to the irregular morphology of the powder used and its larger size. Although the rods produced by SLM exhibits a large amount of pores, a large fracture strain was observed in compression, which is related to the small grain size obtained in the rods.

Acknowledgements

The authors are grateful to B. Bartusch, H. Wendrock e U. Kühn for technical assistance and for the financial support granted by DFG, Germany, and CAPES, Brazil, under the program BRAGECRIM.

References

1. Löber L, Klemm D, Kühn U and Eckert J. Rapid manufacturing of cellular structures of steel or titaniumalumide. *Materials Science Forum*. 2011; 690:103-106. http://dx.doi.org/10.4028/www.scientific.net/MSF.690.103.
2. Shishkovsky I, Morozov Y and Smurov I. Nanofractal surface structure under laser sintering of titanium and nitinol for bone tissue engineering. *Applied Surface Science*. 2007; 254(4):1145-1149. http://dx.doi.org/10.1016/j.apsusc.2007.09.021.
3. Shishkovsky I, Morozov Y and Smurov I. Nanostructural self-organization under selective laser sintering of exothermic powder mixtures. *Applied Surface Science*. 2009; 255(10):5565-5568. http://dx.doi.org/10.1016/j.apsusc.2008.09.090.
4. Lagoudas DC. *Shape memory alloys: modeling and engineering applications*. New York: Springer; 2008. p. 435.
5. Otsuka K and Wayman CM. *Shape memory materials*. Cambridge: Cambridge University Press; 1998. p. 284.
6. Mukunthan K and Brown LC. Preparation and properties of fine grain ß-CuAINi strain-memory alloys. *Metallurgical and Materials Transactions. A, Physical Metallurgy and Materials Science*. 1988; 19A:9.
7. Pauly S, Löber L, Petters R, Stoica M, Scudino S, Kühn U, et al. Processing metallic glasses by selective laser melting. *Materials Today*. 2013; 16(1-2):37-41. http://dx.doi.org/10.1016/j.mattod.2013.01.018.
8. Cava RD, Bolfarini C, Kiminami CS, Mazzer EM, Botta WJ Fo, Gargarella P, et al. Spray forming of Cu–11.85Al–3.2Ni–3Mn (wt%) shape memory alloy. *Journal of Alloys and Compounds*. 2014; 615(Suppl 1):S602-S6. http://dx.doi.org/10.1016/j.jallcom.2013.11.166.
9. Mazzer EM, Kiminami CS, Gargarella P, Cava RD, Basilio LA, Bolfarini C, et al. Atomization and selective laser melting of a Cu-Al-Ni-Mn shape memory alloy. *Materials Science Forum*. 2014; 802:343-348. http://dx.doi.org/10.4028/www.scientific.net/MSF.802.343.
10. Otsuka K, Sakamoto H and Shimizu K. Successive stress-induced martensitic transformations and associated transformation pseudoelasticity in Cu-Al-Ni alloys. *Acta Metallurgica*. 1979; 27(4):585-601. http://dx.doi.org/10.1016/0001-6160(79)90011-7.
11. Sakuma T and Nishizawa T. [title in Japanese]. *Bulletin of the Japan Institute of Metals and Materials*. 1971; 10(5):279-289. http://dx.doi.org/10.2320/materia1962.10.279.
12. Otsuka K and Ren X. Physical metallurgy of Ti-Ni-based shape memory alloys. *Progress in Materials Science*. 2005; 50(5):511-678. http://dx.doi.org/10.1016/j.pmatsci.2004.10.001.